

Examining Contrasting Excitation Modes within Battery Characterisation using Maximum Length Sequences

Andrew Fairweather, Vxl Power Ltd, Station Road, North Hykeham, Lincoln, LN6 3QY, United Kingdom, andrew.fairweather@vxipower.com

David Stone, Electrical Machines and Drives Research Group, Department of Electronic and Electrical Engineering, The University of Sheffield, Mappin Street, Sheffield, S1 4DT, United Kingdom, d.a.stone@sheffield.ac.uk

Martin Foster, Electrical Machines and Drives Research Group, Department of Electronic and Electrical Engineering, The University of Sheffield, Mappin Street, Sheffield, S1 4DT, United Kingdom, m.p.foster@sheffield.ac.uk

Abstract

This paper extends on previous work involving the use of maximum length sequences as tools for parameter estimation within electrochemical batteries[1-4] and comprises a study of the modes of application of a perturbation signal to batteries in the form of discharge, charge and bipolar charge/discharge arrangements driven by a frequency rich signal.

Examinations are made of the contemporary techniques, and by the use of experiments over a range of States-of-Charge, the advantages of each method are presented.

Using a series of experiments, impedance responses are produced using the tests batteries under perturbation from each of the test modes. Analysis of these results under comparative test conditions allows observations to be made regarding the application of each mode, and proposals are made for the complementary inclusion of the test regimes in a hybrid SoC/SoH prediction system.

1. Introduction

Electrochemical cells remain a key enabling technology for the progression of the technologies which are at the forefront of renewable energy and electric vehicles. Measurement of State-of-Function (SoF), State-of-Health (SoH) and State-of-Charge (SoC) of the battery or cell, and in turn, the electrochemical “fuel gauge” are notoriously difficult to realise. SoC reporting methods employing measurement of terminal voltage [5] can be effective if the load is constant, but typically require implementation of an algorithm to allow for cell degradation, whilst existing methods involving Coulomb counting[6] have been successful in consumer electronics, they are often subject to periodic recalibration to maintain accuracy.

Electrochemical cells and batteries employ chemical reactions in order to affect charge storage and delivery of current and as such exhibit different characteristics during charge and discharge [7]. Additionally, a battery at higher SoC accepts additional charge less readily and experiences a characteristic increase in impedance [7]. It follows therefore that applying perturbation signals in different modes could facilitate improved state identification over a range of charge states.

The motivation for this work was therefore focused on investigating then benefits and applicability of a battery perturbation test technique using differing methods (Charge, Discharge and Bipolar) to apply the test signal.

The investigation was concerned with establishing how the methods examined could be applied practically as individual testing schemes, or as a combined three-mode test signal which could be used to identify specific battery states.

2. Pseudo Random Binary Sequences as a perturbation signal

Pseudo Random Binary Sequences (PRBS) offer a digitally generated signal which on inspection appears random in nature, but is actually periodic, and therefore has properties which are extremely useful in several application areas. There are a class of PRBSs termed Maximum Length Sequence (MLS) that exhibit properties similar to white-noise and the sequences have extensively been used to establish audio frequency response[8], and system frequency response analysis generally[9].

A PRBS generator can be seen in figure 1, using shift registers with modulo 2 (XNOR) feedback at predetermined “tap” positions, with the number of shift registers defining the bit order, $n[10]$.

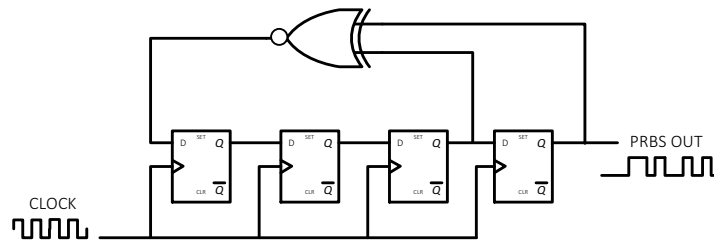


Fig. 1. 4-bit PRBS generator constructed from shift registers with determined “tap” positions and XNOR feedback

2.1. Effects of test current amplitude and voltage thresholds

In the course of previous investigations[1], the selection of test current amplitude was considered in order to achieve an appropriate level of excitation to the test battery. Levels close to the rated capacity (c_r)/20 rate were found to be a good compromise between being intrusive to battery state and providing a reasonable level of voltage information for analysis[11]. Additionally, as the experimental set up was based on a constant current charger, the upper charge voltage limit for this system was very relevant to the battery under test. Charge voltages for the test battery from manufacturer’s data[12] were taken into consideration during the application of the PRBS charge profile (during both charge mode and bipolar tests), as it was important that the battery should not be overcharged. It was decided also that by using the manufacturer’s recommended voltage levels, temperature compensated, observations at near to 100% state of charge could lead to distinct SoC indicators [3].

3. PRBS test investigation

The overall test system block diagram is shown in Fig. 2 with the PRBS test system photograph in Fig. 3.

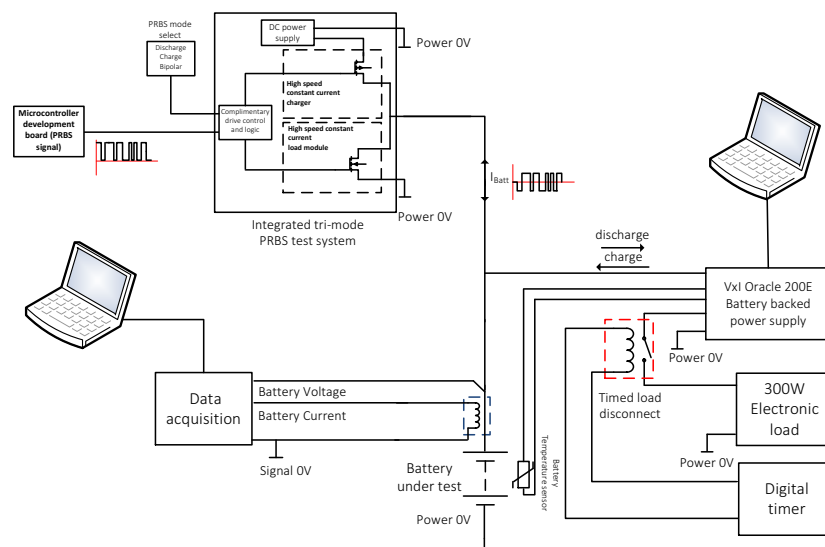


Fig 2. PRBS test system block diagram

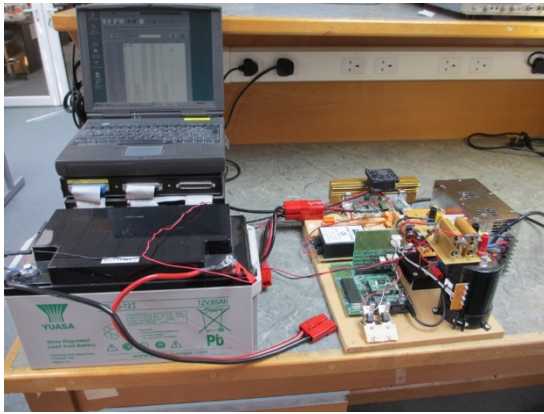


Fig. 3. PRBS test system photograph



Fig. 4. Controlled charge/discharge system photograph

3.1. Test procedure

A controlled charge and discharge system (Fig. 4) was used to remove a pre-determined amount of energy from the test battery, separately to the PRBS system used in applying the test perturbation. Discharge and charge power stages are driven by an amplitude offset drive circuit in order to generate a PRBS perturbation signal centred around zero current. The hardware was configured in order that switching between the 3 modes of test (charge, discharge and bipolar) could be carried out easily.

The battery used during the tests was a 65Ah 12V Valve Regulated Lead Acid (VRLA) (Yuasa NP65-12i) type, which was conditioned with a number of charge and discharge cycles before being charged to 100% SoC using the temperature compensated Lead-Acid charger within the test controlled charge/discharge apparatus (figure 4). The bipolar PRBS was developed with prior work in mind and the test level used was $\pm 4A$, using an extended bandwidth hybrid PRBS sequence. The upper voltage limit for the charge pulse was fixed before the test, using previously established limits for such excitation[3]. PRBS tests (discharge, charge and bipolar) were then carried out on the battery at 100% SoC before it being discharged at 5 amps for 2 hours to remove around 15% of the rated capacity in preparation for the next test at 85% SoC. The third stage was to discharge the battery at the 20 hour discharge rate to the manufacturers specified End-of-Discharge (EoD) Voltage before carrying out the final PRBS test at close to 0% SoC.

3.2. Battery model development

In previous work carried out by the authors in battery characterisation the Randles' model[13] was used, and this was developed during further investigations [3, 4, 14]. These investigations, and examination of the work by Salameh et al[15] led to development of the model shown in Fig. 5 which was used in the analysis.

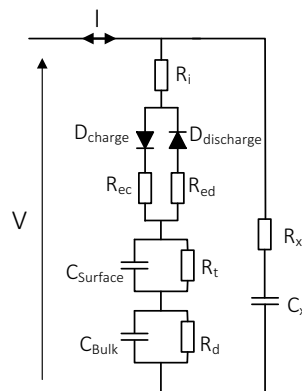


Fig. 5. Developed model

D_{charge} and $D_{\text{discharge}}$ are ideal diodes with no forward volt drop, in series with R_{ec} and R_{ed} respectively which represent the electrolyte resistance[15] which in conjunction with R_i (ohmic resistance) represent the significant series resistance of the battery.

R_x and C_x were used in development of models in the wider part of this research [14] and have been shown to improve the curve fitting of the impedance response to simulation. These parameters represent a parallel branch element of $C_{Surface}$ and R_t which have found to be applicable to this model development.

3.3. Test results

Example current and voltage data are seen in figures 6 and 7 at 85% SoC one of the dynamic charge (PRBS) tests.

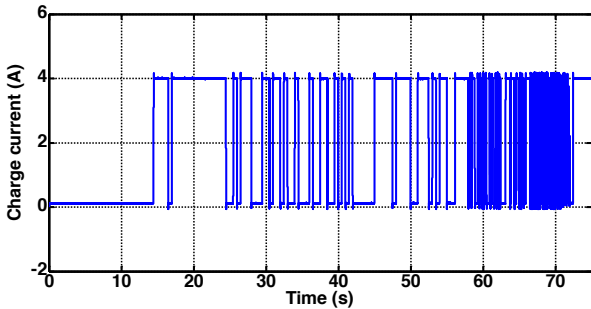


Fig. 6. Current waveform, 85% SoC, charge test

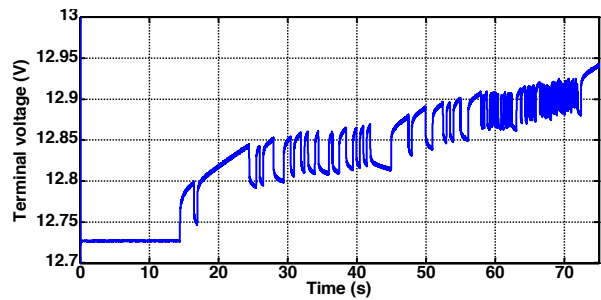


Fig. 7. Voltage response, 85% SoC charge test

Example current and voltage waveforms are seen in figures 8 and 9 for the bipolar test at 85% SoC.

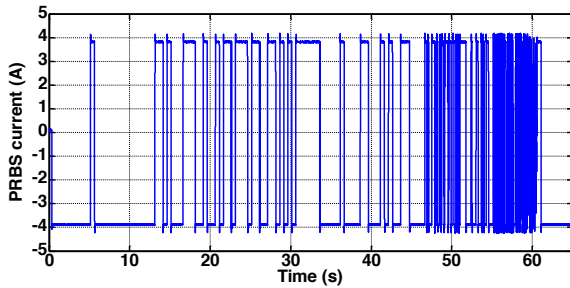


Fig. 8. Bipolar PRBS test current waveform, 85% SoC.

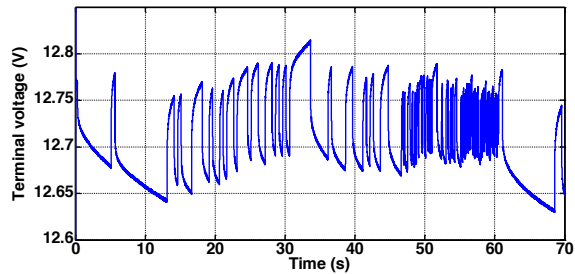


Fig. 9. Bipolar PRBS test voltage response, 85% SoC

The impedance information obtained from the tests are shown in Figs. 10 to 18. Transfer function analysis of the adopted model (Fig. 5) was employed to obtain a curve fit for each of the results.

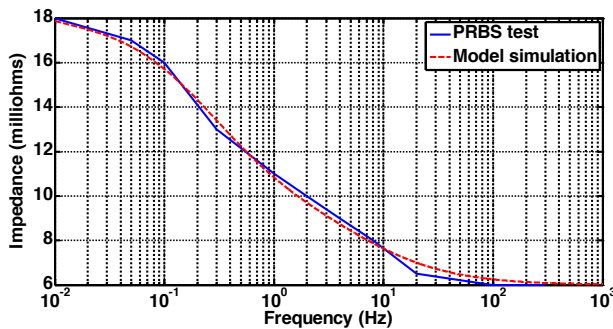


Fig.10. 100% SoC, discharge mode PRBS

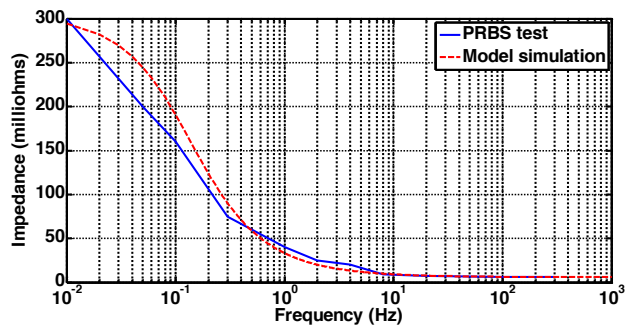


Fig. 11. 100% SoC, charge mode PRBS

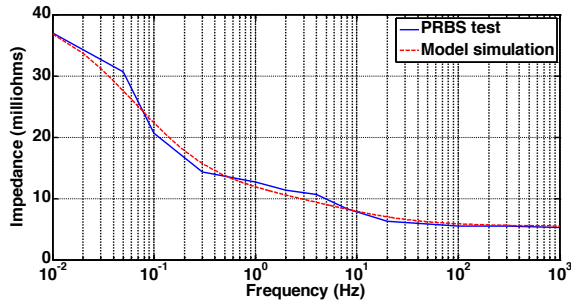


Fig. 12. 100% SoC, Bipolar mode PRBS

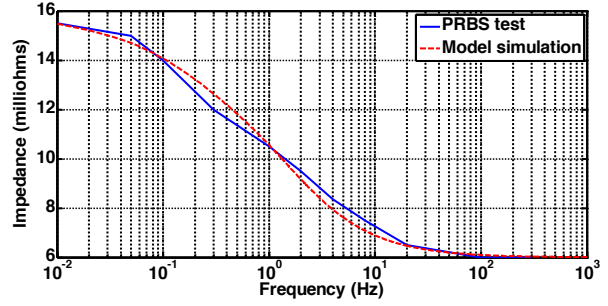


Fig. 13. 85% SoC, discharge mode PRBS

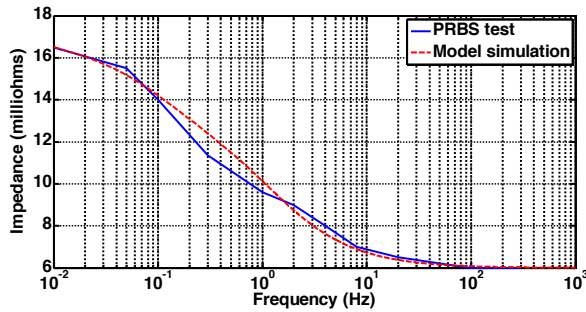


Fig.14. 85% SoC, charge mode PRBS

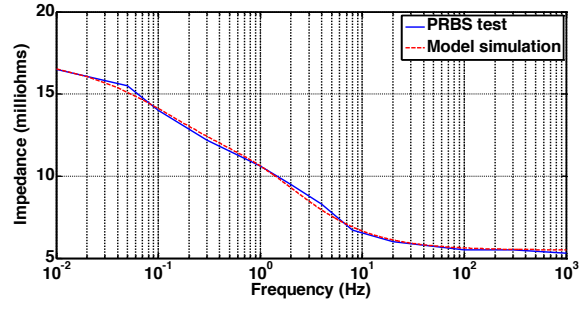


Fig.15. 85% SoC, Bipolar mode PRBS

Figures 10 to 12 illustrate the comparative results at 100% SoC. As mentioned, testing at this state of charge can lead to an indeterminate result, as the battery may not be at a steady state terminal voltage. This has been addressed previously in battery pulse testing by applying a preload to the battery[16], and in PRBS discharge tests by disregarding initial data sets until a pseudo steady-state voltage envelope is observed. However, the PRBS charge technique does not have this facility as the test mode inherently charges the battery. This led to an elevation of terminal voltage during the 100% SoC test which resulted in “clipping” in the PRBS charge current. Importantly, this is observed in figure 11 as the high magnitude of low frequency impedance, whilst the high frequency impedance approaches the expected level. This phenomenon clearly shows detection of end of charge, whilst showing healthy impedance results for the higher frequency part of the response.

Figures 13 and 14 show the test results at 85% SoC for the discharge and charge test modes. Both results show similar results but the differences in the charge and discharge processes are apparent in elements of the curve fitting.

Figure 15 shows the impedance plot for the bipolar test at 85% SoC. This is consistent with the discharge and charge PRBS methods, within the quasi-linear area of operation of the battery. The low frequency impedance of the battery is therefore more representative of typical performance, and the plot generally would be used to indicate battery SoH.

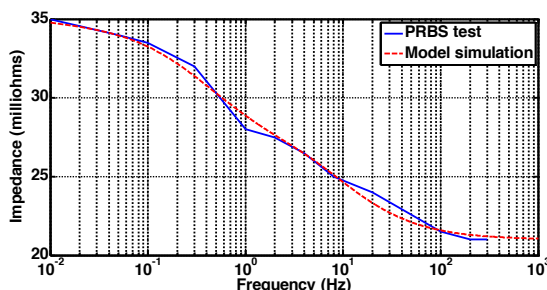


Fig. 16. 0% SoC, discharge mode PRBS

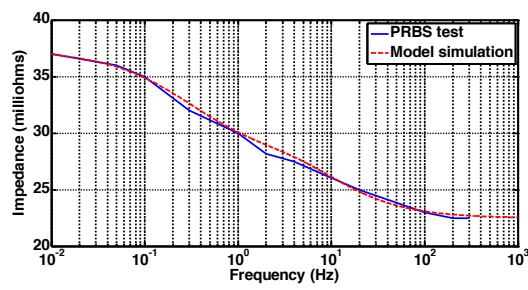


Fig. 17. 0% SoC, charge mode PRBS

Figures 16 and 17 show the discharge test and charge test results for 0% SoC. The battery shows an elevation in impedance across the test frequency range which shows both test modes

exhibit similar results but with some differences for the two test methods over the frequency range, with the discharge mode showing a generally lower impedance.

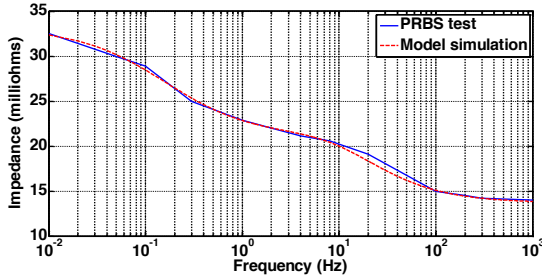


Figure 18. 0% SoC, Bipolar PRBS

Figure 18 shows the bipolar impedance plot for the test at 0% SoC. The battery in this state shows an elevation in impedance across the test frequency range. This gives a distinct indication of a discharged battery and can be compared to the 100% SoC results (Figure 13) which show similarly the increased LF impedance, but preserve the healthy HF result. The test impedance results are presented together in Figs. 19 and 20.

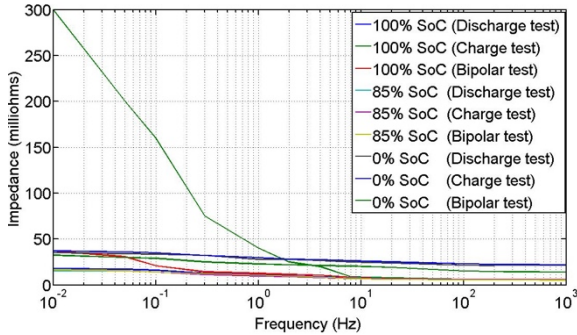


Fig.19. Comparative impedance results

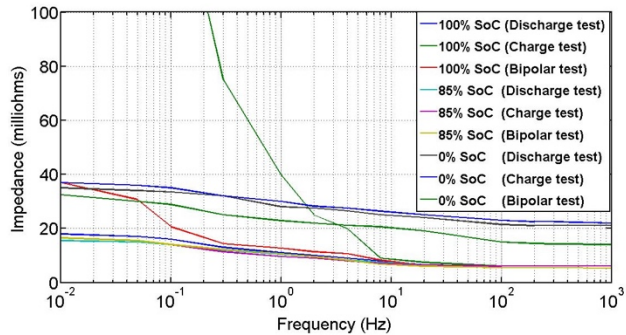


Fig. 20. Expanded scale to show detail

In spite of this observed increase in low frequency impedance, the higher frequency impedance for the battery appears healthy, allowing both SoC and SoH to be reported, provided the upper voltage threshold for the PRBS charge is carefully selected.

3.4. Battery model parameters

Table 1 shows the parameters obtained for the curve fitting using the bipolar tests, with the corresponding discharge and charge test parameters.

R_i , R_{ec} and R_{ed} are combined parameters for the bipolar tests as no distinction can be made between the individual components, and are therefore compared to R_i+R_{ec} for the charge mode tests and R_i+R_{ed} for the discharge mode tests.

At 85% SoC the three modes of test show similarly impedance and parameter results, but it is at the extremes of charge states 0% and 100% where the individual methods show the significant differences.

Across the test methods, the elements of surface capacitance ($C_{Surface}$ and C_x) remain indicators of the ability of the battery to deliver energy, and further profiling of this capacitance against actual discharge tests may reveal direct correlations to bulk capacity.

The results in the table show differences the charge and discharge technique mainly related to the elements of $C_{Surface}$. This demonstrates somewhat the different reactions involved in the charge and discharge processes [7] and overall observations on the validity of the charge technique are satisfied in that clear results are observed for the various charge states as compared to the discharge technique with trends that are recognisable for both methods.

Table 1. Obtained model parameters

BATTERY STATE AND TEST MODE	R_I, R_{EC}, R_{ED} (m Ω)	$R_I + R_{EC}$ (m Ω)	$R_I + R_{ED}$ (m Ω)	R_T (m Ω)	$C_{SURFACE}$ (F)	C_X (F)	R_X (m Ω)
100% (BIPOLAR)	5.5	-	-	35.3	3.9	60	5.8
100% SOC (DISCHARGE)	-	-	6	12	6	34	4
100% SOC (CHARGE)	-	6	-	300	4	2	9
85% (BIPOLAR)	5.5	-	-	11.3	12	60	10
85% SOC (DISCHARGE)	-	-	6	9.5	16	35	9
85% SOC (CHARGE)	-	6	-	10.75	20	60	9
0% (BIPOLAR)	13.7	-	-	19.2	1	31	12.5
0% SOC (DISCHARGE)	-	-	21	13.8	2.5	16	9
0% SOC (CHARGE)	-	22.5	-	14.6	2.5	22	9

4. Conclusion

This work explores the respective benefits of frequency rich signals applied as charge, discharge and bipolar modes to obtain state indicators and equivalent circuit parameters for Lead-Acid batteries.

Applying a perturbation to the test battery as a discharge is the most straightforward method of applying this signal, and produces useful results. Long tests are precluded due to the overall effect on the test battery terminal voltage, but this is a trade off against a straightforward test.

The effect of applying a bipolar PRBS perturbation signal with an average value of zero facilitates longer tests at lower frequency and/or increased bit length. Additionally, the bipolar system was applicable at 100% SoC, and showed repeatable results at this state, with a characteristic, elevated low frequency impedance at the fully charged state.

Within the charge mode PRBS tests, it was discovered that by control of the charge voltage headroom high states of charge were clearly identified, and whilst reporting this SoC, the charge based PRBS was also suitable for reporting SoH, indicating via high frequency impedance the current delivering capability of the battery.

The charge PRBS could be used to measure impedance over the full range of charge and therefore finds application as a state evaluation system that can be incorporated with a battery charger with minimal additional hardware, predominantly requiring an embedded processor to carry out the analysis.

The investigations described within this paper form part of a body of ongoing research by the author and co authors and will lead to further publications in this field.

5. References

1. Fairweather, A.J., M.P. Foster, and D.A. Stone, *Battery parameter identification with Pseudo Random Binary Sequence excitation (PRBS)*. Journal of Power Sources, 2011. **196**(22): p. 9398-9406.
2. Fairweather, A.J., M.P. Foster, and D.A. Stone, *Modelling of VRLA batteries over operational temperature range using Pseudo Random Binary Sequences*. Journal of Power Sources, 2012. **207**(0): p. 56-59.
3. Fairweather, A.J., M.P. Foster, and D.A. Stone, *Application of Maximum Length Sequences to Battery Charge Programming for Parameter Estimation in Lead-Acid Batteries*, in *PCIM Europe 2013*. 2013: Nuremberg, Germany.
4. Fairweather, A.J., M.P. Foster, and D.A. Stone, *Bipolar Mode Pseudo Random Binary Sequence Excitation for Parameter Estimation in Lead-Acid Batteries*, in *PCIM Asia*. 2013: Shanghai, China.
5. Coleman, M., et al., *State-of-Charge Determination From EMF Voltage Estimation: Using Impedance, Terminal Voltage, and Current for Lead-Acid and Lithium-Ion Batteries*. Industrial Electronics, IEEE Transactions on, 2007. **54**(5): p. 2550-2557.
6. Nguyen, K.S., et al., *Enhanced coulomb counting method for estimating state-of-charge and state-of-health of lithium-ion batteries*. Applied Energy, 2009. **86**(9): p. 1506-1511.
7. Linden, D. and T.B. Reddy, *Handbook of batteries*. 4th ed. McGraw-Hill handbooks. 2010, New York: McGraw-Hill. 1 v. (various pagings).
8. Jamieson, D.G. and T. Schneider, *Electroacoustic evaluation of assistive hearing devices*. Engineering in Medicine and Biology Magazine, IEEE, 1994. **13**(2): p. 249-254.
9. Vermeulen, H.J., J.M. Strauss, and V. Shikoana. *On-line estimation of synchronous generator parameters using PRBS perturbations*. in *Power Engineering Society General Meeting, 2003, IEEE*. 2003.
10. Davies, W.D.T., *System identification for self-adaptive control*. 1970, London, New York,: Wiley-Interscience. xiv, 380 p.
11. Fairweather, A.J., D.A. Stone, and M.P. Foster, *Evaluation of UltraBattery™ performance in comparison with a battery-supercapacitor parallel network*. Journal of Power Sources, 2013. **226**(0): p. 191-201.
12. Yuasa Battery Europe. *Yuasa NP Valve Regulated Lead Acid Battery Manual*. NP VRLA Application Manual [Application Manual] 1999 1/12/99; 1:[1, 2, 5, 6, 7, 8, 9, 12, 22, 24, 27, 29]. Available from: <http://www.yuasa-battery.co.uk/industrial/downloads.html>.
13. Fairweather, A.J., M.P. Foster, and D.A. Stone, *VRLA battery parameter identification using pseudo random binary sequences (PRBS)*, in *IET Conference Publications*. 2010. p. TU244.
14. Fairweather, A.J., *State-of-Health (SoH) and State-of-Charge (SoC) Determination in Electrochemical Batteries and Cells Using Designed Perturbation Signals* in *Electronic and Electrical Engineering*. 2015, University of Sheffield: Sheffield, UK.
15. Salameh, Z.M., M.A. Casacca, and W.A. Lynch, *A mathematical model for lead-acid batteries*. Energy Conversion, IEEE Transactions on, 1992. **7**(1): p. 93-98.
16. Coleman, M., W.G. Hurley, and L. Chin Kwan, *An Improved Battery Characterization Method Using a Two-Pulse Load Test*. Energy Conversion, IEEE Transactions on, 2008. **23**(2): p. 708-713.